



Modeling and Optimization of Lead (II) Adsorption by a Novel Peanut Hull-g-Methyl Methacrylate Biopolymer Using Response Surface Methodology (RSM)

Megnolia Chaduka, Upenyu Guyo, Ngceboyakwethu P. Zinyama, Piwai Tshuma & Leah C. Matsinha

To cite this article: Megnolia Chaduka, Upenyu Guyo, Ngceboyakwethu P. Zinyama, Piwai Tshuma & Leah C. Matsinha (2020) Modeling and Optimization of Lead (II) Adsorption by a Novel Peanut Hull-g-Methyl Methacrylate Biopolymer Using Response Surface Methodology (RSM), *Analytical Letters*, 53:8, 1294-1311, DOI: [10.1080/00032719.2019.1702993](https://doi.org/10.1080/00032719.2019.1702993)

To link to this article: <https://doi.org/10.1080/00032719.2019.1702993>



Published online: 18 Dec 2019.



Submit your article to this journal [↗](#)



Article views: 47



View related articles [↗](#)



View Crossmark data [↗](#)

PRECONCENTRATION TECHNIQUES



Modeling and Optimization of Lead (II) Adsorption by a Novel Peanut Hull-g-Methyl Methacrylate Biopolymer Using Response Surface Methodology (RSM)

Megnolia Chaduka^a, Upenyu Guyo^a, Ngceboyakwethu P. Zinyama^a, Piwai Tshuma^a, and Leah C. Matsinha^b

^aDepartment of Chemical Technology, Midlands State University, Gweru, Zimbabwe; ^bDepartment of Chemistry, University of Johannesburg, Johannesburg, South Africa

ABSTRACT

The modeling and optimization of lead (II) adsorption was been characterized on a fabricated peanut hull-g-methyl methacrylate biopolymer. A graft copolymer from agro-based waste was prepared by copolymerizing activated carbon from peanut hulls and methyl methacrylate by the use of benzoyl peroxide as the radical initiator in the presence of an aluminum triflate cocatalyst. A central composite design (CCD) was employed to model batch adsorption experiments and optimize and characterize the influence and interaction of relevant parameters including the pH, contact time, adsorbent dosage, and initial concentration. The optimum conditions for the adsorption process were a pH of 5.7, a contact time of 63.75 min, an adsorbent dosage of 0.2250 g in 50 mL, and initial lead (II) concentration equal to 76.25 mg L⁻¹. Under these conditions, 99.30% of lead (II) was removed from aqueous solution. Isotherm studies demonstrated that the experimental results were in accordance with the Langmuir isotherm model with maximum adsorption capacities of 370.40 and 137.0 mg g⁻¹ in the presence and absence of the cocatalyst, respectively. The experimental results concurred with a pseudo second-order kinetic model that described the adsorption process as chemisorptive. Consequently, the peanut hull-g-methyl methacrylate prepared in the presence of an aluminum triflate cocatalyst has been shown to be potentially effective and sustainable for the remediation of lead (II) from contaminated waters.

ARTICLE HISTORY



Received 20 August 2019
Accepted 6 December 2019

KEYWORDS

Modeling; response surface methodology (RSM); central composite design (CCD); lead (II) adsorption

Introduction

Land, air and water pollution are on the increase in the world due to the growing population and enhanced industrialization (Lin et al. 2019; Zhang et al. 2019). The wastewater released from industrial processes may include toxic substances such as heavy metals and organic substances (Vieira et al. 2018; Gadekar and Ahammed 2019; Khoshnam, Zargar, and Rahimi 2019; Kumar et al. 2019; Okoli and Ofomaja 2019;

CONTACT Upenyu Guyo  upguyo@gmail.com  Department of Chemical Technology, Midlands State University, Private bag 9055, Gweru, Zimbabwe.

Color versions of one or more of the figures in the article can be found online at www.tandfonline.com/lanl.

Trifi et al. 2019). Industries are required to remove these pollutants before their discharge into the environment (Hokkanen, Bhatnagar, and Sillanpää 2016).

Lead is one of the major heavy metals that are non-biodegradable and highly toxic (Lu et al. 2019). Lead (II) occurs in both inorganic and organic forms; the inorganic form enters the body through the inhalation of dust particles, ingestion or through the skin, causing the teratogenic effect (Duruibe, Ogwuegbu and Egwurugwu 2007). Organic lead (II) primarily affects joints, reproductive systems, synthesis of hemoglobin, dysfunctions in the kidneys, cardiovascular system, and acute and chronic damage to the central nervous system (CNS) and peripheral nervous system (PNS) (Huang et al. 2019). The exposure to lead (II) has also been shown to be associated with increases in blood pressure and low sperm count. Lead (II) ions concentrate in the food chain and threaten plants, animals and humans through bioaccumulation in living tissues, water and soil. The maximum acceptable limit for lead (II) in drinking water by the World Health Organization (WHO) is 0.01 mg L^{-1} (Xiong et al. 2019).

Lead (II) removal from wastewaters is important before they interact with plants, animals and human beings. The available methods for the removal of lead (II) ions are expensive and ineffective at low concentrations. These methods include, but not limited to ultra-filtration, chemical precipitation, membrane separation, ion exchange, and electro-dialysis (Hu et al. 2018; Samuel et al. 2018; Huang et al. 2019; Lu et al. 2019). Adsorption techniques using various sorbents have become the technology of choice in remediating contaminated wastewaters. This approach has several merits compared to the other methods that include the ease of regeneration, low cost, enhanced removal efficiency, and selectivity (Mohammad et al. 2019).

Several adsorbents prepared from agricultural and plant materials have been applied for the removal of lead (II) (Georgescu et al. 2018; Hu et al. 2018; Samuel et al. 2018; Awual 2019; Qu et al. 2019; Yan et al. 2019; Yu et al. 2019). The use of natural materials as adsorbents, although increasing, is impaired by bleeding of Colored compounds, odor, and additional pollution by the use of chemicals (Hokkanen, Bhatnagar, and Sillanpää 2016). The use of raw plant materials in water treatment is also limited by bacterial attack and the decomposition of the biomass (El-saied et al. 2012). Hence, there is a need to modify and tailor-make natural adsorbents for the adsorption of pollutants.

In the current study, peanut hulls, which are a waste generated from processing groundnuts, were used as the precursor for the preparation of a novel biopolymer. Raw peanut hulls have poor characteristics such as shrinking and swelling, high affinity for water and low mechanical strength (El-saied et al. 2012) which has impeded their commercial applications. In order to improve the raw peanut hulls, biopolymers were prepared by copolymerizing activated carbon from the peanut hulls with methyl methacrylate using benzoyl peroxide as the radical initiator.

The biopolymers were prepared in the presence and absence of an aluminum triflate cocatalyst. The fabricated biopolymers were employed for the removal of lead (II) from aqueous solution and subsequently from industrial effluents. A commonly used response surface experimental design based on the central composite design (CCD) was employed in this study. The central composite design was composed of thirty experimental measurements that were modeled using Design Expert Software with the

adsorption experiments carried out in the batch mode. The response surface methodology (RSM) was used to evaluate the influence of relevant parameters and their interactions and quadratic effects on the removal of lead (II) ions from aqueous solutions (Deng and Chen 2019; Kumar et al. 2019; Mohammad et al. 2019; Şahan 2019; Trifi et al. 2019; Yan et al. 2019).

Materials and methods

Materials

All reagents were used as received except for methyl methacrylate (MMA, 99%, Sigma Aldrich) which was passed through activated basic aluminum oxide to remove inhibitors. Other reagents included the radical initiator, benzoyl peroxide (BPO, Sigma Aldrich); toluene (99%, Saarchem); aluminum trifluoromethane sulfonate ($(\text{Al}(\text{OTf})_3$, 99.9%, Aldrich); orthophosphoric acid (H_3PO_4 , 85%, Glassworld); methanol (analytical reagent, Glassworld); sodium hydrogen carbonate (NaHCO_3 , Rutland Industries); sodium carbonate (Na_2CO_3 , Merck Chemicals); sodium hydroxide (NaOH , 99.9%, Glassworld); hydrochloric acid (HCl , 32%, Associated Chemical Enterprises); and lead nitrate ($\text{Pb}(\text{NO}_3)_2 \cdot 4\text{H}_2\text{O}$, 99%, Saarchem).

Collection and preparation of the peanut hull activated carbon

The peanut hulls were obtained from a local farm in the Midlands province of Zimbabwe, hand-washed with tap water in order to remove soluble soil, rinsed with deionized water, and dried in an oven at 60°C overnight to remove moisture. The dried hulls were crushed and mixed with concentrated H_3PO_4 acid in a ratio of 1:1 acid:hulls (w/w) and soaked for 24 h at room temperature. The resultant mixture was activated in a muffle furnace at 500°C for 3 h and cooled to room temperature. The cooled material was passed through 500 micron sieves, soaked in sodium bicarbonate, and washed several times with deionized water to remove any residual acid. The resulting peanut hull activated carbon (PHAC) material was dried in an oven at 105°C for 24 h, cooled to room temperature, and stored in a dessicator for additional processing.

Synthesis of the peanut hulls grafted with methyl methacrylate

The peanut hull activated carbon (PHAC) was grafted by the addition of methyl methacrylate (MMA) in a 250 mL three-necked round bottomed flask. First, the PHAC powder was slurried in toluene (20% w/v) by stirring the mixture for 30 minutes from 75 to 80°C before cooling to the polymerization temperature of 70°C (Tsubokawa, Fujiki, and Sone 1988). The flask contents were purged with nitrogen before the introduction of the MMA. The radical initiator, benzoyl peroxide, and the aluminum triflate cocatalyst were added to the flask contents and the reaction was allowed to continue for 2 h at constant temperature with stirring at 400 rpm. The reaction was terminated by addition of ice cold methanol followed by filtration and drying in an oven at 60°C to obtain the peanut hull-g-methyl methacrylate biopolymer.

Characterization of the peanut hull-g-methyl methacrylate biopolymer

Moisture content

The moisture content was determined using the ASTM D 2867-09 oven drying method by weighing 1 g of the peanut hull-g-methyl methacrylate biopolymer and heating for 3 h at a constant temperature of 150 °C followed by cooling in a desiccator. The peanut hull-g-methyl methacrylate biopolymer sample was reweighed after cooling and the percentage difference between the initial weight and the final weight is the moisture content of the peanut hull-g-methyl methacrylate biopolymer.

Ash content determination

The ash content was determined according to the standard ASTM D 2866-70, by weighing the peanut hull-g-methyl methacrylate biopolymer into a porcelain crucible and exposing the material to a constant temperature of 800 °C for 2 h and thereafter cooling in a desiccator. The residue was weighed and a cycle of heating, cooling and weighing was repeated until a constant mass was obtained. The percentage weight of the residue is the ash content.

Volatile matter

The ASTM D5832-98 standard method was used for the determination of the volatile matter. A gram of the biopolymer was heated in a covered crucible of known weight in a furnace at 950 °C for 10 minutes, cooled in a desiccator, and subsequently weighed. The final mass of the biopolymer was determined and the volatile matter is the percentage weight loss.

Fixed carbon content

The fixed carbon content was calculated by subtracting the percentages of moisture, ash content, and volatile matter from 100.

Determination of pH of point zero charge (pH_{zpc})

The salt addition method was used to determine the pH of point zero charge (pH_{zpc}). A solution of 0.1 M NaCl was prepared using cooled distilled water that had been boiled prior to remove dissolved carbon dioxide. To a series of vials, 20 mL of the 0.1 M NaCl solution were added and pH adjusted to 2, 4, 6, 8, 10 and 12 using 0.1 M HCl or 0.1 M NaOH. The peanut hull-g-methyl methacrylate biopolymer (0.05 g) was added into each vial. The vials were capped and solutions stirred for 24 h. The final pH of the solutions was measured.

The difference between the initial and final pH (ΔpH) was plotted against the initial pH. The point at which the curve crosses the line when initial pH is equal to the ΔpH was deemed to be the pH_{zpc} .

Table 1. Experimental variables and their actual levels used for CCD.

	pH	Contact Time (min)	Dosage (g/50 mL)	Initial Concentration (mg/L)
Minimum value	2	5.00	0.10	5.00
Intermediate value	5	122.5	0.35	52.5
Maximum value	8	240	0.60	100

Determination of functional groups

The functional groups present in the solid peanut hull-g-methyl methacrylate biopolymer were identified using a ThermoFischer Scientific (Nicolet 6700, USA) Fourier transform infrared spectrophotometer (FTIR) using a scanning range from 4000 to 400 cm^{-1} . The transmission spectra were recorded as KBr pellets.

Response surface experimental design

The influence and interaction of solution pH, contact time, adsorbent dosage and initial lead (II) concentration on the adsorption of lead (II) from solution were studied using the central composite design. The central composite design composed of 16 factorial points, 8 axial points and 6 center points was obtained using Design Expert software. The independent variables were coded as shown in Table 1. The actual values of the process variables and their levels were established by conducting preliminary ad hoc experiments.

The behavior of the adsorption system was explained by the use of the following general second-order polynomial model (Eq. (1)):

$$q_e = b_0 + b_1X_1 + b_2 X_2 + b_3X_3 + b_4X_4 + b_5X_1X_3 + b_6 X_3X_4 + b_7X_1^2 + b_8X_3^2 + b_9X_4^2 \quad (1)$$

where q_e is the adsorption capacity of the peanut hull-g-methyl methacrylate biopolymer (mg g^{-1}); X_1 is the pH; X_2 is the contact time (min), X_3 is the adsorbent dosage (g), and X_4 is the initial lead (II) concentration (mgL^{-1}).

Batch adsorption studies

Batch adsorption studies were carried out by the addition of appropriate quantities of the peanut hull-g-methyl methacrylate biopolymer into a series of vessels containing 50 mL of lead (II) ions solutions by the central composite design provided in Table 2 (Yu et al. 2019). The required pH of lead (II) solutions was obtained by the addition of 0.1 M HCl or 0.1 M NaOH solutions. The solutions were agitated on a shaker at 150 rpm for a specific time stipulated in the design and passed through Whatman number 42 filter paper. The residual lead (II) ions in the filtrate were determined using a Shimadzu flame atomic absorption spectrophotometer. A total of 30 experimental runs were set up. The lead (II) percentage removal (R) was determined by use of:

$$R = \frac{(C_o - C_e)}{C_o} \times 100 \% \quad (2)$$

Table 2. Full CCD showing four variables, experimental and predicted responses for lead (II) adsorption.

Factor 1	Factor 2	Factor 3	Factor 4	Response 1	Response 2	Predicted Adsorption
A: pH	B: Contact time min	C: Dosage g/50 mL	D: Initial Concentration mg/L	Lead (II) Removal %	Adsorption capacity mgg ⁻¹	capacity mgg ⁻¹
3.5	63.75	0.475	28.75	98.89	2.99	2.97
6.5	181.25	0.225	76.25	99.51	16.86	16.9
5.0	240	0.35	52.5	99.37	7.45	7.46
6.5	181.25	0.475	76.25	99.67	8.00	8.02
5.0	122.5	0.35	52.5	99.30	7.45	7.43
5.0	122.5	0.1	52.5	94.80	24.89	16.5
5.0	122.5	0.35	52.5	99.18	7.44	7.43
5.0	122.5	0.35	100	99.28	14.18	16.8
6.5	181.25	0.475	28.75	99.44	3.01	3.02
5.0	5	0.35	52.5	97.94	7.35	7.4
5.0	122.5	0.35	52.5	99.09	7.43	7.43
3.5	181.25	0.475	28.75	98.26	2.97	2.99
6.5	63.75	0.475	76.25	99.40	7.98	7.99
5.0	122.5	0.35	5	96.00	0.69	1.32
6.5	63.75	0.225	28.75	98.64	6.30	6.34
5.0	122.5	0.35	52.5	99.22	7.44	7.43
5.0	122.5	0.35	52.5	99.24	7.44	7.43
3.5	181.25	0.225	76.25	99.06	16.78	16.8
3.5	63.75	0.225	76.25	98.40	16.67	16.7
3.5	181.25	0.475	76.25	99.63	8.00	7.99
6.5	63.75	0.475	28.75	98.82	2.99	2.99
2.0	122.5	0.35	52.5	94.34	7.08	7.11
5.0	122.5	0.35	52.5	99.03	7.43	7.43
6.5	63.75	0.225	76.25	99.90	16.93	16.9
3.5	63.75	0.225	28.75	98.33	6.28	6.23
6.5	181.25	0.225	28.75	98.92	6.32	6.37
3.5	181.25	0.225	28.75	98.71	6.31	6.26
8.0	122.5	0.35	52.5	97.14	7.29	7.25
3.5	63.75	0.475	76.25	99.57	7.99	7.97
5.0	122.5	0.6	52.5	99.41	4.35	4.35

The adsorption capacity (q_e) of peanut hull-g-methyl methacrylate biopolymer at equilibrium was determined by:

$$q_e = \frac{(C_0 - C_e) V}{M} \quad (3)$$

where q_e is the mass of lead (II) ions adsorbed by the biopolymer at equilibrium (mg g^{-1}), C_0 and C_e are the initial and final lead (II) concentrations in the solution, respectively, in mg L^{-1} , V is the volume of the solution (L), and M is the mass of the employed peanut hull-g-methyl methacrylate biopolymer (g).

Statistical analysis and process model fitting

After the adsorption process, a model equation was proposed and the model was employed to fit the data. Stepwise regression analysis was performed to develop the regression model. Factors with p values greater than 0.05 at 95% confidence interval were removed as their contribution were deemed to be insignificant. The final regression model was obtained after the removal of the insignificant independent variables.

The model was validated by normal probability plots, testing for outliers, and subsequently interpreted by the use of profile plots.

Peanut hull-g-methyl methacrylate biopolymer reusability test

Adsorption-desorption studies were conducted to characterize the potential of regenerating and reusing the peanut hull-g-methyl methacrylate biopolymer. The optimum conditions found after the optimization measurements were used for the desorption of lead (II) ions. A 50 mL lead (II) solution of optimum volume and pH were transferred into labeled bottles and 0.225 g of the peanut hull-g-methyl methacrylate biopolymer were added. The bottles were agitated for 1 h, after which the contents were filtered and the filtrate analyzed for residual metal ions by FAAS. A 50 mL 0.1 M HCl solution was employed to desorb the metal ions from the biopolymer and the resultant solution was analyzed for the desorbed metal ions using FAAS. The adsorption and desorption cycles were repeated a number of times to characterize the reusability of the biopolymer.

Removal of Pb(II) from industrial wastewater

The industrial wastewater samples were collected from a stream near a local mining company in Kadoma, Zimbabwe. The samples were stored in clean plastic bottles prior to their analysis. The predetermined experimental conditions were applied to 50 mL of the industrial wastewater samples for adsorption.

Results and discussion

Characterization of peanut hull-g-methyl methacrylate biopolymer

The assessment of the moisture content, volatile matter and ash content provides a method of evaluating the stability and quality of the peanut hull-g-methyl methacrylate biopolymer as an adsorbent. The ash content and volatile matter influence the activity of the adsorbents and relate to the inorganic element content, with high levels of ash content and volatile matter accounting for low adsorption efficiencies. The ash content and volatile matter in peanut hull-g-methyl methacrylate biopolymer were low, with values of 4.60% and 9.99, respectively, indicating that the fabricated adsorbent was primarily organic matter.

The moisture content was also low (4.08%) showing that it would not dilute the action of the adsorbent. Low percentages of the mentioned attributes indicate a relatively small particle density, which shows that the biopolymer may be extended to be used as an adsorbent in column reactors (Ektepete and Horsfall 2011). The high fixed carbon content (81.33%) showed that peanut hull-g-methyl methacrylate biopolymer is a good and stable adsorbent.

The pH of zero point charge of the peanut hull-g-methyl methacrylate biopolymer was determined to be 5.61. During the batch adsorption studies, pH values lower than the pH_{zpc} were acidic whilst above were basic. The pH of zero point charge shows that removal of lead (II) ions would be optimum at pH values higher than 5.61.

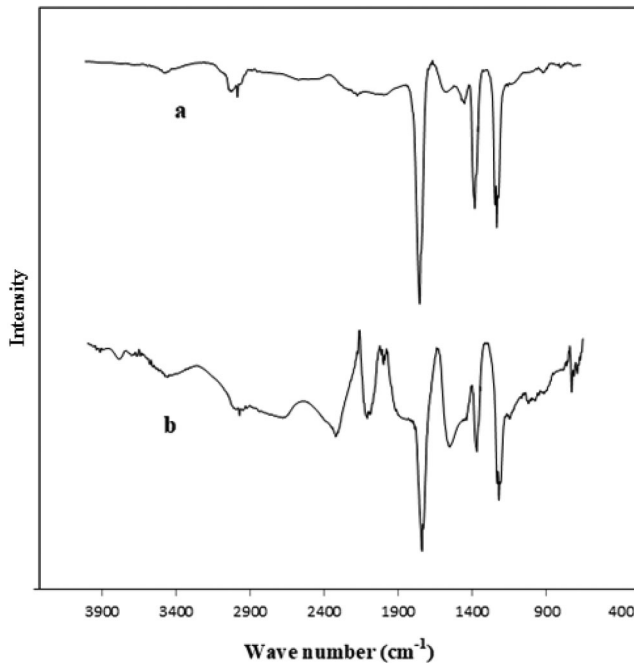


Figure 1. FTIR spectra of (a) peanut hull activated carbon and (b) peanut hull-g-methyl methacrylate biopolymer.

Fourier transform infrared spectroscopy was employed to determine the presence of the functional groups responsible for interaction with the adsorbate. The spectra of raw peanut hulls and the peanut hull-g-methyl methacrylate biopolymer are presented in [Figure 1](#). The peanut hull-g-methyl methacrylate biopolymer spectrum showed a band due to the NH group and a free stretching vibration of OH at 3456 cm^{-1} . A CH stretching vibration was observed at 2924 cm^{-1} . Evidence of grafting is evidenced by compositional changes that are demonstrated by the narrowing of the NH peak. These results show that the NH group participated in the copolymerization reaction.

The broad and intense peak at 1034 cm^{-1} is characteristic of a C-O-C single bond, while the peaks at 1728 and 2988 cm^{-1} are caused by C=O and C-H bonds in poly(methyl methacrylate), respectively ([Guyo et al. 2017](#)). The peak between 2300 and 2200 is characteristic of an isocyanate group (N=C=O) vibration.

Statistical analysis and process model fitting

The batch adsorption experiments were conducted according to a central composite design which evaluated the effect of four process parameters: solution pH, contact time, adsorbent dosage and initial lead (II) concentration in thirty (30) experimental runs. The experimental independent variables, their levels and the response variables, are presented in [Table 2](#).

The experimental measurements were fitted to the general second order polynomial model ([Eq. \(1\)](#)) following a step-wise regression analysis. All of the insignificant terms

Table 3. ANOVA for the response surface reduced quadratic model for lead (II) adsorption.

Source	Sum of squares	Mean square	F-value	p-value
Model	439.69	48.85	28,996.12	<0.0001
A-pH	0.027	0.027	16.13	0.0009
B-Contact time	4.55×10^{-3}	4.55×10^{-3}	2.7	0.1186
C-Dosage	147.17	147.17	87,348.25	<0.0001
D-Concentration	240.53	240.53	1.43×10^5	<0.0001
AC	7.28×10^{-3}	7.28×10^{-3}	4.32	0.0531
CD	30.35	30.35	18,012.27	<0.0001
A ²	0.098	0.098	58.26	<0.0001
C ²	6.49	6.49	3849.8	<0.0001
D ²	0.83	0.83	494.36	<0.0001
Residual	0.029	1.69×10^{-3}		
Lack of fit	0.028	2.36×10^{-3}	42.16	0.0003
Pure error	2.80×10^{-4}	5.61×10^{-5}		
Coefficient of determination, R ²	0.9999			
Adjusted R ²	0.9999			
Adequate Precision	557.036			

(p -value > 0.05) were disregarded to give the final regression equation in terms of coded factors:

$$q_e = 7.43 + 0.034X_1 + 0.014X_2 - 3.03X_3 + 3.88X_4 - 0.021X_1X_3 - 1.38X_3X_4 - 0.062X_1^2 + 0.75X_3^2 + 0.41 X_4^2 \quad (4)$$

where q_e is the response variable (adsorption capacity); X_1 is pH, X_2 is contact time in min, X_3 is adsorbent dosage in g, and X_4 is initial Pb(II) concentration.

An analysis of variance (ANOVA) test was conducted to determine the statistical significance of the model and model terms (linear, square and interaction parts) as well as the difference between the observed and the predicted responses (Şahan 2019). Table 3 shows the parameters that are used to show the adequacy of the model. In addition, the predicted R² value was comparable to the adjusted R² (difference less than 0.2) showing good correlation between the experimental and predicted responses. The ANOVA test showed that the coefficient of determination (R²) of the regression model was 0.9999, meaning that 99.99% of variation in the observed data is explained by the model.

Regression model validation

Before the model was used to analyze the results, model validation was carried out to determine the adequacy of the model in interpreting the experimental measurements. The model was validated based on the normal probability plot, the plot of standard residual versus predicted response, a check for outliers, and the correlation between observed and predicted values. Figure 2a shows that the residuals are randomly scattered around the zero line with no particular pattern showing a normal behavior of the residuals. In addition, the plot shows that there were no outliers which are points falling outside the range indicated by the red horizontal lines. Figure 2b shows that a strong correlation existed between the predicted and experimental data as demonstrated by the data points being close or falling on the oblique line. Overall, these characteristics

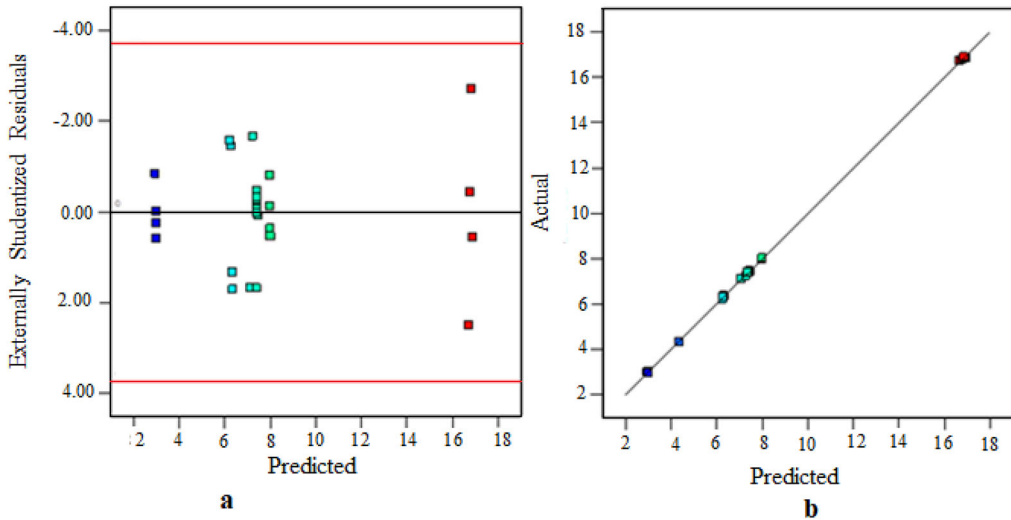


Figure 2. Plot of (a) residuals and predicted values and (b) correlation of actual and predicted values.

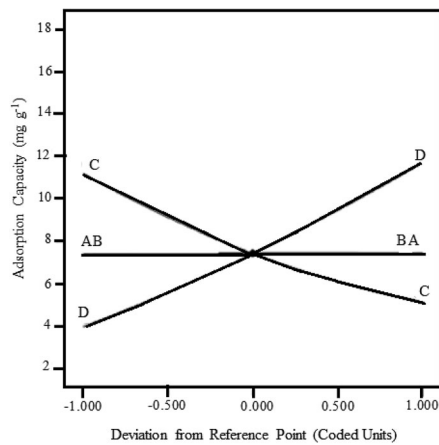


Figure 3. Perturbation plots of the employed model.

showed that the model was statistically valid and may be used confidently to analyze and characterize the experimental data.

Perturbation and three dimensional response surface plots

The effects of the individual process variables on adsorption capacity were explained using the perturbation plot and the response surface plots (Yan et al. 2019). Figure 3 shows the perturbation plot obtained using the Design Expert software. The perturbation plot shows that the pH (X_1) and contact time (X_2) had no significant influence on the lead (II) adsorption efficiency. An increase in the adsorbent dosage (X_3) resulted in a decrease in lead (II) adsorption capacity, while adsorption capacity was enhanced by an increase in the initial lead (II) concentration. The decrease in adsorption capacity

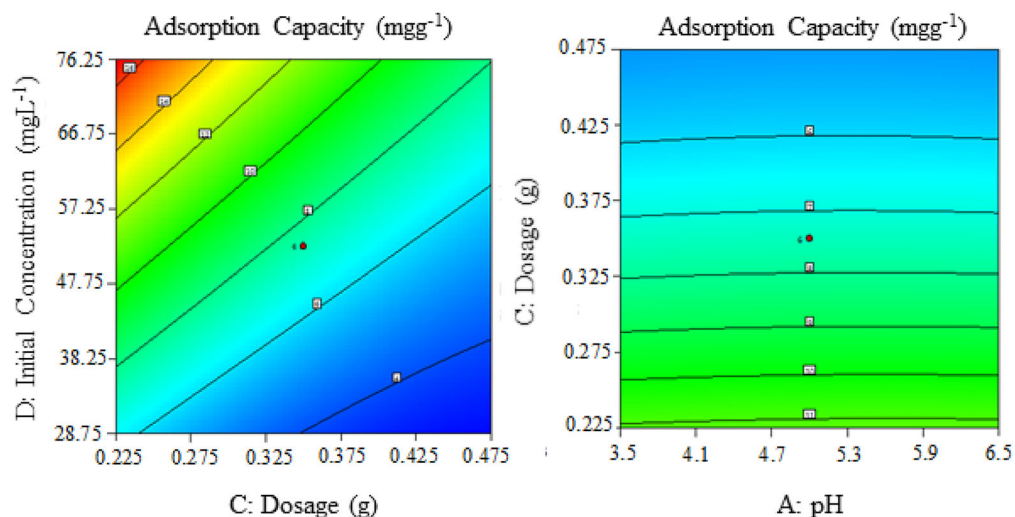


Figure 4. Adsorption capacity as a function of (a) adsorbent dosage and initial concentration at pH 5 and a contact time of 122.5 min and (b) pH and adsorbent dosage at a contact time of 122.5 min and an initial concentration of 52.5 mg L^{-1} .

may be attributed to the overlap in the active adsorption sites on the surface of the adsorbent as the mass of the adsorbent is increased.

The perturbation plots are complemented by the three dimensional response surface plots that demonstrate the mutual effects of two process variables on the adsorption as the other two factors are held constant (Yan et al. 2019). Figure 4a shows that the mutual effect of the adsorbent dosage and initial lead (II) concentration on adsorption capacity (q_e) while the pH and contact time are constant. An increase in the adsorption capacity as the initial lead (II) concentration is enhanced may be attributed to the increased driving force of the mass transfer and the occupation of vacant active sites on the adsorbent.

The contour plots of the polynomial equation with respect to mutual effect of pH and adsorbent dosage are shown in Figure 4b. This figure shows that the influence of pH is insignificant and that a low adsorbent dosage favors higher adsorption. In the study, the solution pH was restricted between 3.5 and 6.5, as above pH 6.5, a hydroxide precipitate is formed.

Prediction and validation of the optimum process conditions

The desirability function on the Design Expert software was used to examine the optimum conditions for the lead (II) adsorption (Khalifa et al. 2019; Kumar et al. 2019; Mohammad et al. 2019). The criteria used to obtain a maximum adsorption capacity occurred when contact time and adsorbent dosage were minimized when the initial lead (II) concentration was a maximum and pH was maintained in the range from 3.5 to 6.5. The optimum conditions at pH 5.7, contact time 63.75 minutes, adsorbent dosage 0.2250 g in 50 mL and initial lead (II) concentration 76.25 mgL^{-1} were predicted to remove 99.57% of lead (II) from aqueous solution. The predicted experimental

Table 4. Langmuir and Freundlich parameters for lead (II) adsorption.

Isotherm	Parameter	PH-g-MMA – with catalyst	PH-g-MMA – without catalyst
Langmuir	Maximum adsorption capacity, q_{\max} (mg g^{-1})	370.4	137.0
	Equilibrium Langmuir constant, b	0.00041	0.00096
	Chi-squared, χ^2	0.215	0.198
	Coefficient of determination, R^2	0.9904	0.9995
Freundlich	Adsorption capacity, K_f	8.6395	1.05
	Intensity of adsorption, n	1.07	1.13
	Chi-squared, χ^2	3.078	0.675
	Coefficient of determination, R^2	0.9905	0.9989

conditions were validated by conducting triplicate experiments using the conditions. The optimization revealed that the experimental lead (II) removal was 99.66% with a standard deviation of 0.34%. Consequently, the validity and the adequacy of the model developed using the RSM approach was verified.

Adsorption isotherms

Freundlich (Freundlich 1906) and Langmuir (Langmuir 1918) models were used to analyze the isotherms of lead (II) adsorption on the peanut hull-g-methyl methacrylate biopolymer. Freundlich and Langmuir models are described by the following linear equations:

$$\ln q_e = \frac{1}{n} \ln C_e + \ln K_f \quad (5)$$

$$\frac{C_e}{q_e} = \frac{C_e}{q_{\max}} + \frac{1}{b q_{\max}} \quad (6)$$

where q_e is the mass of lead (II) (mg g^{-1}) adsorbed onto the peanut hull-g-methyl methacrylate biopolymer at equilibrium, q_{\max} (mg g^{-1}) is the maximum adsorption capacity, b is the equilibrium Langmuir constant, C_e (mg L^{-1}) is the equilibrium concentration, and K_f (mg g^{-1}) and n are constants representing the adsorption capacity and intensity of adsorption, respectively.

The results shown in Table 4 indicate that the Langmuir model better fitted the adsorption measurements compared to the Freundlich model. The conclusion was reached based on higher R^2 values and lower chi-squared (χ^2) values for Langmuir model relative to those of the Freundlich model. The mechanism of adsorption assumed by the Langmuir isotherm model is localized monolayer adsorption of lead (II) on the peanut hull-g-methyl methacrylate biopolymer surface. The calculated values of the Freundlich constant n were 1.07 and 1.13 showing that the adsorption processes were favorable ($1 < n < 10$).

Comparison of the maximum adsorption capacities of various adsorbents

Table 5 shows the results of the comparison of maximum lead (II) adsorption capacities of various adsorbents. The peanut hull-g-methyl methacrylate biopolymer had

Table 5. Comparison of maximum lead (II) adsorption capacities of various adsorbents.

Adsorbent	Maximum adsorption capacity (mg g ⁻¹)	Reference
Carboxylated cellulose nanocrystal sodium alginate hydrogel beads	223.2	Hu et al. (2018)
Modified Walnut Shell	221.24	Li, Zeng, and Xue (2019)
Hazelnut hulls	13.05	Imamoglu and Tekir (2008)
Coconut shells	26.51	Sekar, Sakthi, and Rengaraj (2004)
Ball milled wheat straw	134.68	Cao et al. (2019)
Polyaniline coated sisal fibers composite	6.53	Teklu, Wangatia, and Alemayehu (2019)
Chitosan modified persimmon tannin composite	179.3	Li, Wang, et al. (2019)
Amino-functionalized magnetic aerobic granular sludge composite	127.0	Huang et al. (2019)
Peanut hull-g-methyl methacrylate (PH-g-MMA) – with catalyst	370.4	This study
Peanut hull-g-methyl methacrylate (PH-g-MMA) – without catalyst	137.0	This study

satisfactorily high adsorption efficiency and better adsorption capacity compared to other adsorbents.

Adsorption kinetics

In the present work, a kinetic study was conducted in order to investigate the potential mechanism and the rate controlling steps of lead (II) adsorption onto the peanut hull-g-methyl methacrylate biopolymer. The pseudo-first order (Lagergren 1898) and pseudo-second order (Ho and McKay 1999) kinetic models were fitted to the experimental kinetic measurements. The mathematical expressions for the pseudo-first order model and pseudo-second order models are shown in their linear forms as

$$\ln (q_e - q_t) = \log q_e - \frac{t \cdot k_1}{2.3} \quad (7)$$

$$\frac{t}{q_t} = \frac{t}{q_e} + \frac{1}{k_2(q_e)^2} \quad (8)$$

where q_e and q_t are the masses of Pb(II) adsorbed onto the peanut hull-g-methyl methacrylate biopolymer (mg g⁻¹) at equilibrium and at time t , respectively; k_1 (min⁻¹) is the rate coefficient for the pseudo-first-order kinetic model, t is the time (min), and k_2 is the equilibrium pseudo-second order kinetic model rate constant (g mg⁻¹ min⁻¹).

The suitability of the models to describe the kinetics of the adsorption process were evaluated based on the coefficients of determination (R^2) and the agreement between experimental q_e and calculated q_e values. Based on these criteria, the best model should have a higher R^2 and a closer agreement between experimental q_e and calculated q_e values. Table 6 presents the kinetic parameters which demonstrate that the kinetics measurements best fitted the pseudo-second order kinetic model. The assumptions that follow based on the pseudo-second order kinetic model are that the rate limiting step is dependent on the concentrations of lead (II) and the biopolymer and that the chemical reaction between the lead (II) and the biopolymer is significant in the rate limiting step.

Table 6. Kinetic models parameters for lead (II) adsorption.

	Pseudo first-order model			Pseudo second-order model			
	Experimental adsorbed lead (II) at equilibrium (mg g^{-1})	Calculated adsorbed lead (II) at equilibrium (mg g^{-1})	Kinetic model rate constant (min^{-1})	Coefficient of determination, R^2	Calculated adsorbed lead (II) at equilibrium (mg g^{-1})	Kinetic model rate constant ($\text{g mg}^{-1} \text{min}^{-1}$)	Coefficient of determination, R^2
Adsorbent in catalyst	7.457	0.045	0.0099	0.8951	7.456	0.423	0.999
Adsorbent without catalyst	7.453	0.0002	0.0099	0.8951	7.456	0.327	0.999

Table 7. Peanut hull-g-methyl methacrylate biopolymer repeated adsorption-desorption cycles.

Cycle	Lead (II) removal (%)
1	98.82 ± 0.22
2	98.20 ± 0.88
3	95.11 ± 1.54
4	94.62 ± 2.01
5	92.52 ± 0.77
6	90.54 ± 0.45
7	88.12 ± 0.97
8	85.35 ± 2.45
9	79.63 ± 1.72

Adsorption thermodynamics

Thermodynamic parameters, which include standard Gibb's free energy change (ΔG°), enthalpy change (ΔH°), and the entropy change (ΔS°), were determined in order to evaluate the thermodynamic nature of adsorption of lead (II) onto PH-g-MMA. The parameters were obtained using the following equations:

$$\Delta G^\circ = -RT \ln K_d \quad (9)$$

$$K_d = \frac{q_e}{C_e} \quad (10)$$

$$\Delta G^\circ = \Delta H^\circ - T\Delta S^\circ \quad (11)$$

$$\ln K_d = \frac{\Delta S^\circ}{R} - \frac{\Delta H^\circ}{RT} \quad (12)$$

where R is the ideal gas constant, T is the absolute temperature (K), K_d is the thermodynamic equilibrium constant, q_e is the equilibrium amount of lead (II) adsorbed (mg L^{-1}) and C_e is the equilibrium concentration of lead (II) (mg L^{-1}). The ΔH° and ΔS° were estimated from the slope and the intercept of the plot of $\ln K_d$ versus $1/T$, respectively. The ΔG° values were -5.66 , -5.05 , -5.43 , and $-5.82 \text{ kJ mol}^{-1}$ at 293.15, 303.15, 313.15, and 323.15 K, respectively. The negative ΔG° values demonstrated that the adsorption process was feasible and spontaneous. The positive ΔH° ($+6.66 \text{ kJ mol}^{-1}$) shows the endothermic nature of the adsorption process, while the positive ΔS° ($+0.0386 \text{ kJ mol}^{-1}$) reflected that there was randomness at the solid/solution interface.

PH-g-MMA reusability test

The fabricated adsorbent, PH-g-MMA was subjected to nine adsorption-desorption cycles to characterize its reusability for possible commercial application. It was noted that even after 9 cycles, PH-g-MMA was able to remove more than 75% of the lead (II) from aqueous solution (Table 7).

Removal of Pb(II) from industrial wastewater

The optimized adsorption conditions were applied for the adsorption of lead (II) from industrial wastewaters collected from a local chemical industry. Four wastewater samples were collected and analyzed for lead (II) prior and after adsorption at a value of pH

5.7, a contact time of 63.75 min, and a 0.2250 g dosage of the peanut hull-g-methyl methacrylate biopolymer. The results show an average removal of $97.64 \pm 0.87\%$. The results suggest that peanut hull-g-methyl methacrylate biopolymer has the potential for commercial application for lead (II) adsorption and may have applications for other heavy metals.

Conclusion

This study demonstrated that the fabricated peanut hull-g-methyl methacrylate biopolymer was able to serve as a highly effective and recyclable adsorbent for the removal of lead (II) ions from aqueous solutions and industrial effluents. Moreover, it offers a higher adsorption capacity of 370.40 mg g^{-1} with easy recovery by filtration and a favorable lifetime of over nine adsorption-desorption cycles. The adsorption data fitted well with a Langmuir adsorption isotherm and the pseudo-second order kinetic models demonstrate the adsorption of lead (II) ions onto PH-g-MMA was through a monolayer chemisorption process. Consequently, the peanut hull-g-methyl methacrylate biopolymer may be used as potential material for the removal of lead (II) ions from industrial wastewaters.

Conflict of interest statement

The authors have no conflicts of interest.

References

- Awual, R. 2019. Innovative composite material for efficient and highly selective Pb (II) ion capturing from wastewater. *Journal of Molecular Liquids* 284:502–10. doi:10.1016/j.molliq.2019.03.157.
- Cao, Y., W. Xiao, G. Shen, G. Ji, Y. Zhang, C. Gao, and L. Han. 2019. Carbonization and ball milling on the enhancement of Pb (II) adsorption by wheat straw: Competitive effects of ion exchange and precipitation. *Bioresource Technology* 273:70–6. doi:10.1016/j.biortech.2018.10.065.
- Deng, S., and Y. Chen. 2019. A study by response surface methodology (RSM) on optimization of phosphorus adsorption with nano spherical calcium carbonate derived from waste. *Water Science & Technology* 79 (1):188–97. doi:10.2166/wst.2019.048.
- Duruibe, J. O., M. O. C. Ogwuegbu, and J. N. Egwurugwu. 2007. Heavy metal pollution and human biotoxic effects. *International Journal of Physical Science* 2:112–8.
- Ekpete, O. A., and M. Horsfall Jr. 2011. Preparation and characterization of activated carbon derived from fluted pumpkin stem waste (*Telfairia occidentalis* Hook F). *Research Journal of Chemical Sciences* 1 (3):10–7.
- El-Saied, H., A.H. Basta, M.E. Hassanen, H. Korte, and A. Helal. 2012. Behaviour of rice-by-products and optimizing the conditions for production of high performance natural fiber polymer composites. *Journal of Polymers and the Environment* 20 (3):838–47. doi:10.1007/s10924-012-0439-0.
- Freundlich, H. 1906. Over the adsorption in solution. *Journal of Physical Chemistry* 57:385–471.
- Gadekar, M. R., and M. M. Ahammed. 2019. Modelling dye removal by adsorption onto water treatment residuals using combined response surface methodology-artificial neural network approach. *Journal of Environmental Management* 231:241–8. doi:10.1016/j.jenvman.2018.10.017.
- Georgescu, A., F. Nardou, V. Zichil, and I. D. Nistor. 2018. Adsorption of lead (II) ions from aqueous solutions onto Cr-pillared clays. *Applied Clay Science* 152:44–50. doi:10.1016/j.clay.2017.10.031.

- Guyo, U., N. Matewere, K. Matina, B. C. Nyamunda, and M. Moyo. 2017. Preparation of poly (methyl methacrylate)-grafted *Hyparrhenia hirta* for methyl red removal from colored solutions. *Bioremediation Journal* 21 (3–4):163. doi:10.1080/10889868.2017.1337710.
- Ho, M., and G. McKay. 1999. Pseudo-second order model for sorption processes. *Process Biochemistry* 34 (5):451–65. doi:10.1016/S0032-9592(98)00112-5.
- Hokkanen, S., A. Bhatnagar, and M. Sillanpää. 2016. A review on modification methods to cellulose-based adsorbents to improve adsorption capacity. *Water Research* 91:156–73. doi:10.1016/j.watres.2016.01.008.
- Hu, Z.-H., A. M. Omer, X.-K. Ouyang, and D. Yu. 2018. Fabrication of carboxylated cellulose nanocrystal/sodium alginate hydrogel beads for adsorption of Pb (II) from aqueous solution. *International Journal of Biological Macromolecules* 108:149–57. doi:10.1016/j.ijbiomac.2017.11.171.
- Huang, X., D. Wei, X. Zhang, D. Fan, X. Sun, B. Du, and Q. Wei. 2019. Synthesis of amino-functionalized magnetic aerobic granular sludge-biochar for Pb (II) removal: Adsorption performance and mechanism studies. *Science of the Total Environment* 685:681–9. doi:10.1016/j.scitotenv.2019.05.429.
- Imamoglu, M., and O. Tekir. 2008. Removal of copper (II) and lead (II) ions from aqueous solutions by adsorption on activated carbon from a new precursor hazelnut husks. *Desalination* 228 (1–3):108–13. doi:10.1016/j.desal.2007.08.011.
- Khalifa, E. B., B. Rzig, R. Chakroun, H. Nouagui, and B. Hamrouni. 2019. Application of response surface methodology for chromium removal by adsorption on low-cost biosorbent. *Chemometrics and Intelligent Laboratory Systems* 189:18–26. doi:10.1016/j.chemolab.2019.03.014.
- Khoshnam, F., B. Zargar, and M. Rahimi. 2019. Adsorption and removal of ametryn using graphene oxide nano-sheets from farm waste water and optimization using response surface methodology. *Journal of the Iranian Chemical Society* 16 (7):1383. doi:10.1007/s13738-019-01621-6.
- Kumar, N., M. Angela, S. Palas, and R. Biswajit. 2019. Optimization study of adsorption parameters for removal of Cr (VI) using *Magnolia* leaf biomass by response surface methodology. *Sustainable Water Resources Management* 5 (4):1627–39. doi:10.1007/s40899-019-00322-5.
- Lagergren, S. 1898. Zur theorie der sogenannten adsorption gelöster stoffe. *Veternskapsakad Handlingar* 24:1–39.
- Langmuir, I. 1918. The adsorption of gases on plane surfaces of glass, mica and platinum. *Journal of the American Chemical Society* 40 (9):1361–403. doi:10.1021/ja02242a004.
- Li, S., Z. Zeng, and W. Xue. 2019. Adsorption of lead ion from aqueous solution by modified walnut shell: Kinetics and thermodynamics. *Environmental Technology* 40 (14):1810–20. doi:10.1080/09593330.2018.1430172.
- Li, X., Z. Wang, H. Liang, J. Ning, and G. Li. 2019. Chitosan modification persimmon tannin bioadsorbent for highly efficiency removal of Pb (II) from aqueous environment: The adsorption equilibrium, kinetics and thermodynamics. *Environmental Technology* 40 (1):112–24. doi:10.1080/09593330.2017.1380712.
- Lin, Z., X. Weng, L. Ma, B. Sarkar, and Z. Chen. 2019. Mechanistic insights into Pb (II) removal from aqueous solution by green reduced graphene oxide. *Journal of Colloid and Interface Science* 550:1–9. doi:10.1016/j.jcis.2019.04.078.
- Lu, M., Y. Zhang, Y. Zhou, Z. Su, B. Liu, G. Li, and T. Jiang. 2019. Adsorption-desorption characteristics and mechanisms of Pb (II) on natural vanadium, titanium-bearing magnetite-humic acid magnetic adsorbent. *Powder Technology* 344:947–58. doi:10.1016/j.powtec.2018.12.081.
- Mohammad, A., S. Karamipour, A. Vafaei, and M. Mehdi. 2019. Optimization and modeling of simultaneous ultrasound-assisted adsorption of ternary dyes using copper oxide nanoparticles immobilized on activated carbon using response surface methodology and artificial neural network. *Ultrasonics Sonochemistry* 51:264–80. doi:10.1016/j.ultsonch.2018.10.007.
- Okoli, C. P., and A. E. Ofomaja. 2019. Development of sustainable magnetic polyurethane polymer nanocomposite for abatement of tetracycline antibiotics aqueous pollution: Response surface methodology and adsorption dynamics. *Journal of Cleaner Production* 217:42–55. doi:10.1016/j.jclepro.2019.01.157.

- Qu, J., T. Song, J. Liang, X. Bai, Y. Li, Y. Wei, S. Huang, L. Dong, and Y. Jin. 2019. Adsorption of lead (II) from aqueous solution by modified *Auricularia* matrix waste: A fixed-bed column study. *Ecotoxicology and Environmental Safety* 169:722–9. doi:10.1016/j.ecoenv.2018.11.085.
- Şahan, T. 2019. Application of RSM for Pb (II) and Cu (II) adsorption by bentonite enriched with e SH groups and a binary system study. *Journal of Water Process Engineering* 31:100867. doi:10.1016/j.jwpe.2019.100867.
- Samuel, M. S., S. Sheriff, J. Bhattacharya, K. Subramaniam, and N. D. P. Singh. 2018. Adsorption of Pb (II) from aqueous solution using a magnetic chitosan/graphene oxide composite and its toxicity studies. *International Journal of Biological Macromolecules* 115:1142–50. doi:10.1016/j.ijbiomac.2018.04.185.
- Sekar, M., V. Sakthi, and S. Rengaraj. 2004. Kinetics and equilibrium adsorption study of lead(II) onto activated carbon prepared from coconut shell. *Journal of Colloid and Interface Science* 279 (2):307–13. doi:10.1016/j.jcis.2004.06.042.
- Teklu, T., L. M. Wangatia, and E. Alemayehu. 2019. Removal of Pb (II) from aqueous media using adsorption onto polyaniline coated sisal fibers. *Journal of Vinyl and Additive Technology* 25 (2):189–97. doi:10.1002/vnl.21652.
- Trifi, I. M., B. Trifi, E. B. Souissi, and B. Hamrouni. 2019. Response surface methodology for dyes removal by adsorption onto alginate calcium. *Environmental Technology*. doi:10.1080/09593330.2019.1612470.
- Tsubokawa, N., K. Fujiki, and Y. Sone. 1988. Radical grafting from carbon black. Graft polymerisation of vinyl monomers initiated by peroxyester groups introduced onto carbon black surface. *Polymer Journal* 20 (3):213–20. doi:10.1295/polymj.20.213.
- Vieira, R. M., P. B. Vilela, V. A. Becegato, and A. T. Paulino. 2018. Chitosan-based hydrogel and chitosan/acid-activated montmorillonite composite hydrogel for the adsorption and removal of Pb + 2 and Ni + 2 ions accommodated in aqueous solutions. *Journal of Environmental Chemical Engineering* 6 (2):2713–23. doi:10.1016/j.jece.2018.04.018.
- Xiong, C., S. Wang, W. Sun, and Y. Li. 2019. Selective adsorption of Pb (II) from aqueous solution using nanosilica functionalized with diethanolamine: Equilibrium, kinetic and thermodynamic. *Microchemical Journal* 146:270–8. doi:10.1016/j.microc.2019.01.005.
- Yan, B., Z. Hiew, L. Yee, K. Chiew, S. Gan, S. Thangalazhy-Gopakumar, G. Pan, and T.C. Yang. 2019. Adsorptive decontamination of diclofenac by three-dimensional graphene- based adsorbent: Response surface methodology, adsorption equilibrium, kinetic and thermodynamic studies. *Environmental Research* 168:241–53. doi:10.1016/j.envres.2018.09.030.
- Yan, S., Y. Cai, H. Li, S. Song, and L. Xia. 2019. Enhancement of cadmium adsorption by EPS-montmorillonite. *Environmental Pollution* 252:1509–18. doi:10.1016/j.envpol.2019.06.071.
- Yu, J., S. Zhu, P. Chen, G. Zhu, X. Jiang, and S. Di. 2019. Adsorption behavior and mechanism of Pb (II) on a novel and effective porphyrin-based magnetic nanocomposite. *Applied Surface Science* 484:124–34. doi:10.1016/j.apsusc.2019.04.075.
- Yu, Q., H. Zhao, H. Zhao, S. Sun, X. Ji, M. Li, and Y. Wang. 2019. Preparation of tobacco-stem activated carbon from using response surface methodology and its application for water vapor adsorption in solar drying system. *Solar Energy* 177:324–36. doi:10.1016/j.solener.2018.11.029.
- Zhang, J., J. Shao, Q. Jin, Z. Li, X. Zhang, Y. Chen, S. Zhang, and H. Chen. 2019. Sludge-based biochar activation to enhance Pb (II) adsorption. *Fuel* 252:101–8. doi:10.1016/j.fuel.2019.04.096.